Grounding system impedance influence on the surge arrester frequency-dependent model parameters using PSO-GWO algorithm

Masume Khodsuz
Faculty of Electrical and Computer Engineering, University of Science and Technology of Mazandaran, Behshahr, Iran, and
Valiollah Mashayekhi
Department of Electrical Engineering, Shahrood University of Technology, Shahrood, Iran

Received 8 July 2022
Revised 22 November 2022
16 January 2023
24 January 2023
Accepted 24 January 2023

Abstract

Purpose – This paper aims to focus on the inclusion of the frequency behavior of grounding system effect on surge arrester (SA) model parameters' estimation.

Design/methodology/approach – The grounding system impedance and its frequency behavior are the factors that have influence on the SA performance. Up to now, the grounding system impedance effect and the frequency behavior of the soil parameters have not been studied for the estimation of the parameters of the SA frequency-dependent model. In this paper, the grounding system's influence on the SA dynamic model has been simulated for rod- and counterpoise-shaped electrodes. Particle swarm optimization with a grey wolf optimization algorithm has been implemented as an optimization algorithm to adjust the parameters of the SA dynamic model.

Findings – The results show that the frequency behavior of the grounding impedance and soil electrical parameters can impress the optimum parameters of the SA frequency-dependent model and should be considered for more reliable results. Also, the results evidence that the proposed optimization method provides more accurate results compared to other optimization methods.

Originality/value – To the best of the authors' knowledge, this work is one of the first attempts to investigate the effect of frequency grounding system on SA frequency-dependent model parameters.

Keywords Grounding system impedance, Surge arrester dynamic model, Residual voltage, PSO-GWO algorithm

Paper type Research paper

1. Introduction

To improve the lightning performance of the transmission grids and failure rate diminishing, surge arresters (SAs) have been connected to critical points such as substations and transmission lines. SA is a device to protect electrical equipment from overvoltage transients caused by external (lightning) or internal (switching) events; hence, physical and electrical characteristics election of SAs and energy absorption capabilities are involved in lightning overvoltage limitation. The accurate placement and the determination of the electrical characteristics of the arresters organize critical issues that involve appropriate theoretical substantiation. This is reached by implementing simulation procedures,

COMPEL - The international journal for computation and mathematics in electrical and electronic engineering

0332-1649
DOI 10.1108/COMPEL-07-2022-0229

precision of which depends on the used equivalent circuit models (Bedoui and Bayadi, 2019; Jacqmaer *et al.*, 2009; Li *et al.*, 2021; Zhao and Magoulès, 2012; Zhou *et al.*, 2020). Suitable equivalent models have been represented by many researchers to compute the SA residual voltage for fast-front current waves (Fernandez and Diaz, 2001; Pinceti and Giannettoni, 1999; Application of Surge Protective Devices Subcommittee, 2023). IEEE, Fernandez–Diaz and Pinceti models have been widely used for SA behavior simulation. In IEEE model, two sections of nonlinear resistances are divided by an R-L filter which has very little impedance for slow-front surges and the two nonlinear resistances are in parallel. For fast-front surges, the R-L filter impedance is significant and leads to a current distribution between the two nonlinear sections (IEEE Group, 1992).

In Fernandez–Diaz model, it should be noted that the current ratio is constant over all of the ranges of protection characteristic voltage. With this additional constraint, the voltage increase between the input terminals depends only on the inductance which is obtained using the selection curves of percent increment in the residual voltage for various values of inductance (Fernandez and Diaz, 2001). In the Pinceti model, compared to the IEEE model, the capacitance is eliminated and there is one resistance (about 1-M) between the input terminals to avoid numerical oscillations (Pinceti, 2014). In fact, the last two proposed models are based on the IEEE model, with various parameter calculation processes. The precision of each model is very extremely influenced by the parameter values adjustment.

In response to these challenges, several iteration approaches have been exploited to predict the parameter values of the SA dynamic model (Bayadi, 2008; Christodoulou *et al.*, 2010a, 2010b; Christodoulou *et al.*, 2011; Christodoulou *et al.*, 2010a, 2010b; Lira *et al.*, 2009; Martinez and Durbak, 2005; Nafar *et al.*, 2012, 2011; Sengmanivanh *et al.*, 2021; Vahidi *et al.*, 2008; Zeinoddini-Meymand *et al.*, 2013). An objective function based on the integral of squares of measured errors, which is the error between simulated residual voltage and the obtained residual voltage from 8/20 μs impulse current, has been introduced in Lira *et al.* (2009). Procedures for appropriate parameter estimation and mathematical representation have been represented in Martinez and Durbak (2005). An optimization method based on the genetic algorithm (GA) has been introduced in Bayadi (2008) to achieve the best probable collection of parameter values for SA models. In this method, the comparison of residual voltage simulated curve with an experimentally measured voltage curve is essential. Other approaches based on Powell's optimization or GA are represented in Christodoulou *et al.* (2010a, 2010b), in which the peak of the residual voltage has been used to yield objective function for optimization goal. GA is developed in Christodoulou *et al.* (2011) and Vahidi *et al.* (2008) to evaluate the metal oxide SA circuit model parameters.

The metal oxide SAs failure probability valuation has been introduced in Christodoulou *et al.* (2010a, 2010b), which uses the equivalent circuit models. A developed optimization technique has been used for SA parameters estimation in Nafar *et al.* (2011, 2012). In addition, in these references, a comparison has been drawn among the various V-I characteristic assigning methods of the SA. An improved self-adaptive particle swarm optimization (PSO) algorithm has been established in Zeinoddini-Meymand *et al.* (2013) to estimate SA model parameters. The best set of SA parameters have been calculated under lightning, switching and steep-front impulses. An optimization method based on the downhill simplex method has been introduced in Christodoulou *et al.* (2011). These mentioned methodologies can be proved very valuable, for the accurate SA dynamic model plays an important role in achieving more precise and reliable results in transient analysis and lighting performance studies.

One of the most imperative parameters which has considerable influences on lightning overvoltages is the grounding system impedance. Up to now, the frequency behavior of the grounding systems has not been considered in the dynamic model of the SA to estimate parameter values of the SA. As the real ground connection has a significant resistance

(Christodoulou *et al.*, 2014; Khodsuz, 2022; Sajadi *et al.*, 2020; Shariatinasab *et al.*, 2017; Shariatinasab and Gholinezhad, 2017), the appropriate modeling of an SA is significant. It is obvious that the use of the optimum parameter values in the equivalent circuit models reduces the error between the manufacturer's and the simulated residual voltage significantly, something which is really very important because the arresters models can be more reliable for the insulation coordination studies representing more efficiently the arresters' behavior and resulting in more precise analysis. Within the context alluded above, the inclusion of frequency model of grounding system for the SA parameters should be considered. The method of moments (MoM) can be used as an effective method to solve the electric field integral equation. This method governs the current distribution along grounding system conductors. The MoM is a rigorous, full-wave numerical technique for solving open-boundary electromagnetic problems. Using this technique, you can analyze electromagnetic radiation, scattering and wave propagation problems with relatively short computation times and modest computing resources (Sheshyekani *et al.*, 2014).

This paper aims to evaluate the grounding system impedance effect on the estimation of SA model parameters. To assess the SA model parameters, the transient models of SA with and without considering grounding system impedance have been simulated using MATLAB software. The simulations of the SA dynamic model have been linked to a developed program that is based on particle swarm optimization with a grey wolf optimization (PSO-GWO) algorithm. Parameter determination of different SA models has been performed for ideal and frequency-dependent grounding system models. The grounding system has been simulated for different soil resistivities and also for various grounding electrodes including rod and counterpoise. The validity and accuracy of estimated parameters have been evaluated by comparing the simulated residual voltage and the manufacture's values. The relative error values for the IEEE, Pinceti and Fernandez models have been diminished after optimization compared to their initial values for all simulated grounding systems. The results show that the frequency behavior of the grounding system affects the calculated optimum values of the SA parameters. Consequently, the SA parameters have been calculated more accurately when the frequency behavior of the grounding system is considered in the dynamic model. In addition, the optimized parameters are different for counterpoise-shaped and rod-shaped grounding system which shows the effect of the grounding system type on the SA optimized parameters.

2. Modeling the grounding system and metal oxide surge arrester

In this section, the frequency-dependent model of the SA has been investigated and modeled in MATLAB software.

2.1 Metal oxide surge arrester modeling

The SA models have been represented in the supplementary file (as Figure A). The represented model of IEEE Working Group 3.4.11 includes five parameters (R_0, R_1, L_0, L_1, C). In this model, the inductance dedicated to magnetic fields in the surrounding of the SA has been modeled as the inductance L_0. To stabilize the numerical integration, R_0 has been used during the IEEE model implementation on a computer program. In this model, the inductance L_1 and the resistance R_1 comprise the filter between the two nonlinear resistances (the nonlinear resistances A_0 and A_1). The arrester terminal-to-terminal capacitance has been modeled as C in the represented model.

Simpler forms of the IEEE model have been presented by the other two models. There is no capacitance in the Pinceti–Giannettoni model. However, this model has one resistance at

the input terminals (Application of Surge Protective Devices Subcommittee, 2023). The resistor R is used to avoid numerical oscillations when running the model with a digital program. In the Fernandez–Diaz model, L_0 has been neglected and L_1 has been used to separate the nonlinear resistors A_0 and A_1 (Fernandez and Diaz, 2001). The SA terminal-to-terminal capacitance that has been demonstrated by C is in the arrester model (Fernandez and Diaz, 2001). The resistor R is used to avoid numerical oscillations.

2.2 Grounding system model

The effective circuit modeling of SAs and their parameters adjusting are critical problems for lightning performance and insulation coordination studies. A key objective is to provide a method for the adjustment of the parameters of the circuit models to achieve a more precise demonstration of their dynamic behavior. The results precision of each model is strongly dependent on its adjusted parameters. For this, several iteration methods have been proposed to set the parameter values to minimize the error between the simulated residual voltage and the manufacturer's one (Christodoulou *et al.*, 2010a, 2010b; Christodoulou *et al.*, 2011; Vahidi *et al.*, 2008). Unfortunately, the exact model of the grounding system has been disregarded in previous researches, and the grounding system has been assumed as an ideal ground. So, grounding system is necessary to adjust the parameters of the SAs' circuit models.

Rod-shape and counterpoise-shape are two grounding systems consisting of one or several buried vertical and horizontal conductors. These two kinds of grounding systems have been modeled in this paper. The length of the grounding rod is 6 m, with a circular cross-sectional radius of 8 mm. The counterpoise is one-port 8 m × 8 m, with the burial depth and the radius of 1 m and 8 mm, respectively.

To solve the electric field integral equation solutions, the moment's method is used in the frequency domain. For this purpose, the grounding system is estimated to thin wires that are divided into small segments. To calculate the longitudinal current distribution, the tangential electric field is calculated on each section surface due to each current sample placed in the conductor's axis. This current can be estimated to a constant value, piecewise sinusoidal or a ramp function. The current distribution along grounding conductors and the electric field within the solution domain are calculated by the electric field integral equation solving. The voltage rise at the excitation port can be then easily obtained as a line integration over the electric field along a prespecified path. Finally, the system impedance is formed by the voltage and current values (Sheshyekani *et al.*, 2014; Visacro *et al.*, 2011). After that, to get a transfer function of a certain order, vector fitting is applied to approximate the frequency response. It is able to identify the state space models directly from the frequency domain responses of any single or multiple input–output systems. The system transfer function can be represented as the sum of partial fractions that each one can be modeled as a branch circuit with a specific admittance value. Finally, the synthesized circuit is made by the parallel-connected branches.

Owing to this fact, the soil conductivity and relative permittivity show a frequency-dependent behavior over the frequency range. Because all the computation in the moment's method are performed in the frequency domain, the frequency dependency of the soil parameters is easily inserted in the calculation. As shown in equation (1), the model proposed by Longmire and Smith (1975) is used to model frequency-dependent soil electrical parameters:

$$\rho_0 = 125\left(\frac{p}{10}\right)^{-0.54} \quad (\Omega.m)$$

$$\rho(f) = \left(\rho_0^{-1} + 2\pi\varepsilon_0 \sum_{n=1}^{14} \frac{a_n \left(\left(\frac{p}{10}\right)^{1.28}.10^{n-1}\right)\left(\frac{f}{\left(\frac{p}{10}\right)^{1.28}.10^{n-1}}\right)^2}{1+\left(\frac{f}{\left(\frac{p}{10}\right)^{1.28}.10^{n-1}}\right)^2}\right)^{-1} \tag{1}$$

$$\varepsilon_r(f) = \varepsilon_\infty + \sum_{n=1}^{14} \frac{a_n}{1+\left(\frac{f}{\left(\frac{p}{10}\right)^{1.28}.10^{n-1}}\right)^2},$$

where f is the frequency ranging from dc to 2 MHz; $\varepsilon_r(f)$ and $\rho(f)$ are the relative permittivity and soil resistivity, respectively; ρ_0 is the low-frequency resistivity; p is the water percentage of soil; and a_n are coefficients (Longmire and Smith, 1975). It should be noted that the calculation has been done for soil resistivities 100, 250, 500, 1000 and 3000 Ω m. These three values correspond to water percentages $p = 11.6\%$, $p = 2.77\%$, $p = 0.767\%$, $p = 0.213\%$ and $p = 0.028\%$. In all cases, the ε_∞ is considered 5. The synthesized circuit and the impedance amplitudes for rod grounding system topologies and different soil resistivities are shown in Figure 1 (counterpoise-shaped circuit has been shown as Figure B in the supplementary file).

3. Formulation of the optimization problem

There are different parameters in the three considered models due to which their quantity may have different values. Five parameters exist in the IEEE model (R_0, R_1, L_0, L_1, C), and the Pinceti-Gianettoni model and the Fernandes–Diaz model have three parameters (R_0, L_0, L_1) and (R_0, L_0, C), respectively. The minimization of the relative error has been proposed as an objective function.

The parameters (R, L, C) of each model form a column vector as follows:

$$\begin{aligned} &x = [x_1, x_2, x_3, x_4, x_5]^T = [R_0, R_1, L_0, L_1, C]^T \\ &(\text{IEEE model}) \\ &x = [x_1, x_2, x_3]^T = [R_0, L_0, L_1]^T \\ &(\text{Pinceti} - \text{Gianettoni model}) \\ &x = [x_1, x_2, x_3]^T = [R_0, L_0, C]^T \\ &(\text{Fernandes} - \text{Diaz model}) \end{aligned} \tag{2}$$

The optimal values x_i will be found by applying an optimization algorithm. Minimizing the relative error is the optimization goal which has been calculated as follows:

$$e = \left|\frac{V_s - V_m}{V_m}\right| \tag{3}$$

where V_s is the simulated residual voltage peak value and V_m is the measured one.

The behavior of individuals of bird swarms is the basis of the PSO algorithm. An individual in the swarm tries to approach the optimum through its present velocity, previous experience and the experience of its neighbors or an entire population. These particles are moved around in the search space according to their present velocity, previous

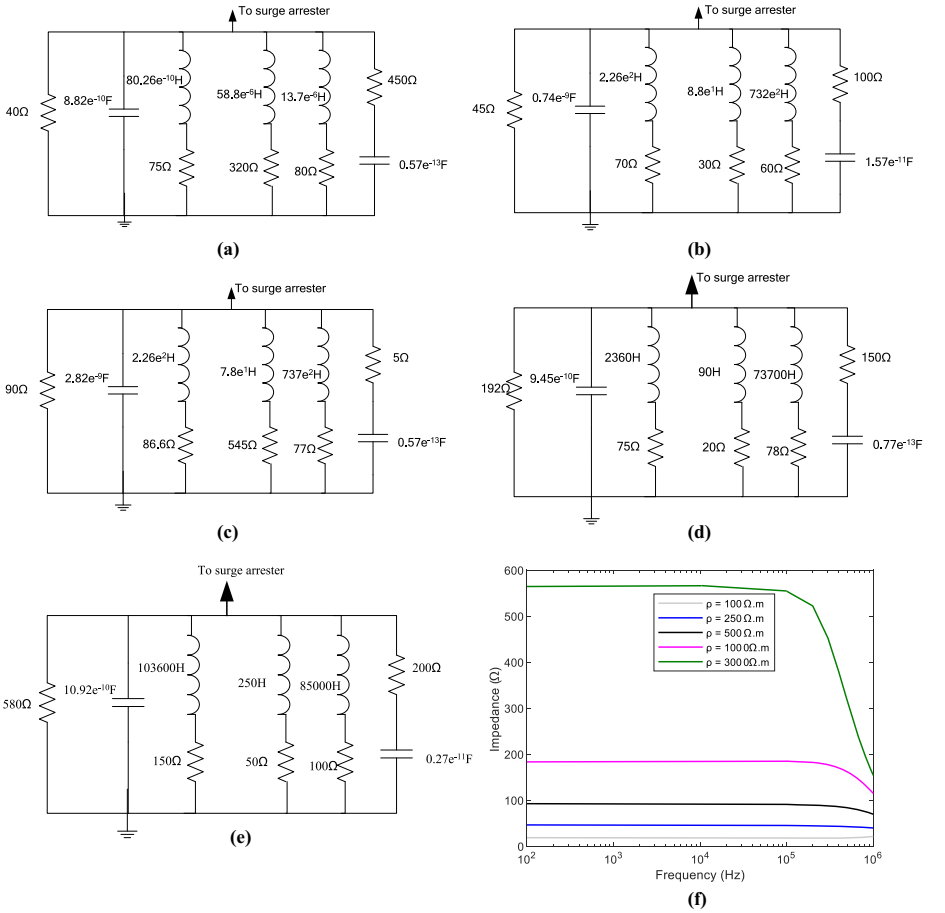

Figure 1.
Rod grounding system model

Notes: (a) $\rho = 100\ \Omega$ m; (b) $\rho = 250\ \Omega$ m; (c) $\rho = 500\ \Omega$ m; (d) $\rho = 1000\ \Omega$ m; (e) $\rho = 3000\ \Omega$ m; (f) self-impedances of the vertical rod

experience and the experience of their neighbors. When improved positions are being discovered, these will then come to guide the movements of the swarm. PSO algorithm permits swarms to profit from their previous experiences, and it is an interesting feature of PSO (Gaing, 2003; Longmire and Smith, 1975; Niknam *et al.*, 2010).

This method has many advantages including simple implementation and adjusting a few parameters. However, this algorithm may trap into a local minimum. Recently, numerous techniques have been reported to overcome this disadvantage by using the hybridization of PSO with other global optimization algorithms (Esmin *et al.*, 2005; Pal *et al.*, 2016; Rokbani *et al.*, 2013). Esmin *et al.* (2005) introduced a new hybrid algorithm called PSO-GWO by combining the PSOs utilization ability with GWO's exploration capability. A hybrid approach has been formulated by combining PSO and GWO algorithms that produce effective and fruitful results. Therefore, in this paper, the hybrid technique of PSO-GWO has been used to generate the best solutions.

3.1 Particle swarm optimization

In the PSO method, particle swarms have the absolute authority to transfer in a multidimensional search space, and the velocity of each particle has been updated as follows (Gaing, 2003; Niknam *et al.*, 2010):

$$v_i^{k+1} = \omega v_i^k + c_1 rand_1 \left(p_{i,pbest}^k - x_i^k \right) + c_2 rand_2 \left(p_{i,gbest}^k - x_i^k \right) \tag{4}$$

where ω is the inertia weight varying in the range of 0.4 to 0.9. c_1 and c_2 are acceleration factors and $rand_1$ and $rand_2$ are random parameters that vary between [0,1]. $p_{i,pbest}$ is the best previous experience of the ith swarm particle, and the best experience between the total population has been shown as $p_{i,gbest}$. The swarm location updating process is according to equation (5):

$$x_i^{k+1} = x_i^k + v_i^{k+1} \tag{5}$$

3.2 Grey wolf optimization

The GWO is a technique based on swarm intelligence which is influenced by the social behavior of grey wolves and based on their hunting strategy. GWO is categorized into four types of wolves. An alpha wolf has a major role in generating new solutions. The second and third levels near alpha wolves have been called beta and delta wolves. The beta wolves guide the leader wolves to make decisions. Response to the alpha has been performed by the delta wolves. Finally, the lowest ranking of wolves has been introduced as omega wolves (Faris *et al.*, 2018; Mahapatra *et al.*, 2019; Mirjalili *et al.*, 2014).

The hunting pattern of grey wolves contains three steps:

(1) approaching prey hounding;

(2) aggressively surrounding the prey until it stops moving; and

(3) attacking the prey.

To mathematically model the behavior of surrounded prey, the following equations are proposed:

$$\begin{aligned} D &= |C.\mathrm{X}_P(t) - \mathrm{X}(t)| \\ X(t+1) &= |X_P(t) - A.D| \end{aligned} \tag{6}$$

where t is the iterations' number, the prey positions have been shown by X_P and X is the gray wolf location. A and C are the coefficient vectors given as follows:

$$\begin{aligned} A &= x\,(2r_1 - 1) \\ C &= 2r_2 \end{aligned} \tag{7}$$

With iterations increasing, the value of x decreases linearly from 2 to 0. The parameters r_1 and r_2 are random numbers in the range of [0, 1]. The updating equation consists of the movement of other wolves in accordance with the three best wolves' position as given by:

$$\begin{aligned} D_\alpha &= |C_1 \mathrm{X}_\alpha - \mathrm{X}| \\ D_\beta &= |C_2 \mathrm{X}_\beta - \mathrm{X}| \\ D_\delta &= |C_3 \mathrm{X}_\delta - \mathrm{X}| \end{aligned} \tag{8}$$

where D_α, D_β and D_δ are the adapted distance between the alpha, beta and delta positions to the other wolves. C_1, C_2 and C_3 are the coefficient factors which are represented in equation (4). If the best values in each iteration were X_1, X_2 and X_3, then the updated prey position would be calculated based on the mean position as given below:

$$\begin{aligned} X_1 &= |X_\alpha - a_1 D_\alpha| \\ X_2 &= |X_\beta - a_2 D_\beta| \\ X_3 &= |X_\delta - a_3 D_\delta| \\ X(t+1) &= \frac{X_1 + X_2 + X_3}{3} \end{aligned} \tag{9}$$

3.3 Particle swarm optimization–grey wolf optimization

The PSO-GWO algorithm has been developed without changing the general operation of the PSO and GWO algorithms. GWO and PSO hybridization integrates the investigation ability of GWO into PSO, and better-produced positions can be made for particles. On the other hand, GWO keeps an equilibrium between investigation and utilization and employs to support the PSO algorithm to diminish the possibility of falling into a local trapping. The investigation capability of the GWO algorithm is used to avoid these risks by leading some particles to positions that are partially improved by the GWO technique instead of directing them to random positions. Thus, hybrid PSO-GWO uses both the advantages of PSO and GWO algorithms. By the PSO-GWO implementation, the solution time may increase, but the developed and improved global searching capability of the hybrid method covers the extended time and consequently improves the convergence. The pseudocode of PSO-GWO algorithm is as follows:

```
1: Imaxiter the number of maximum iterations set by the user
2: Imaxpso the number of maximum PSO iterations set by the user
3: PS: the number of population sizes set by the user
4: procedure PSO-GWO
5: Initialize particles
6: for i = 1 to Imaxpso do
7: for j = 1 to PS do
8: Run standard PSO
9: Update the velocity and the position of current particle
10: if Ipso = Imaxpso then
11: Set x, A, C values
12: Run standard GWO
13: Update the position of α, β, δ wolves
14: Update x, A, C values
15: position of current particle = mean of the positions of three
best wolves
16: end if
17: end for
18: end for
19: end procedure
```

4. Proposed method

The frequency-dependent model of the grounding system has been taken into account to predict the arrester residual voltage under injected current impulse. The flowchart of the PSO-GWO algorithm has been shown in Figure 2. As shown in Figure 2, during optimization, the peak value

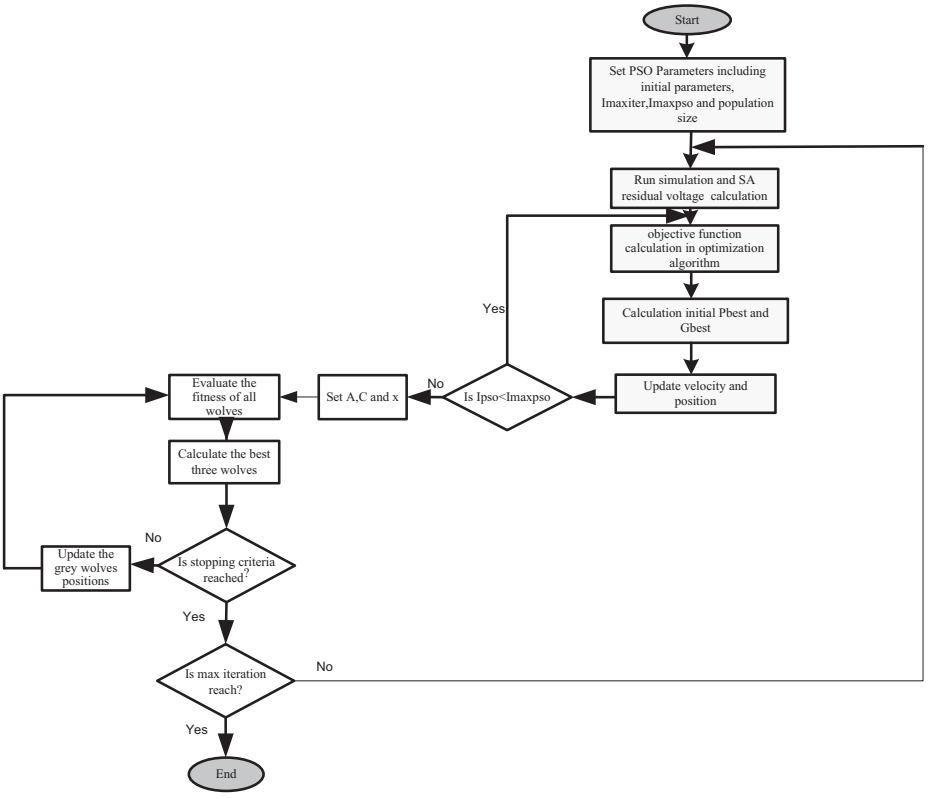

Figure 2.
The surge arrester frequency model optimization flowchart based on PSO-GWO algorithm

of the SA residual voltage has been calculated by the simulated model in MATLAB software for each model of the SA (Simulink section), and then it has been transferred to the PSO-GWO program for the objective function evaluation. This process continues to find the optimum values of each model parameter. The objective function has been proposed based on the error minimization between simulated residual voltage and the manufacture's value. The objective function has been represented as follows:

$$Objective\ Function = \left| \frac{V_s - V_m}{V_m} \right| \tag{10}$$

where V_s and V_m are the simulated and measured residual voltage peak values, respectively.

5. Simulation results

A 150 kV SA simulation has been done using the MATLAB software based on the three SA models. The information of the studied SA has been given in Table 1. Table 2 represents the computed primary values of SA model parameters for 10 kA 8/20 μs injected current. These parameters have been calculated according to the equation mentioned in Fernandez and Diaz (2001), Pinceti and Giannettoni (1999) and Application of Surge Protective Devices Subcommittee (2023).

The best-obtained solutions by the objective function optimization and for 100 Ω m soil resistivities have been summarized in Table 3. The obtained results for 250, 500, 1000 and 3000 Ω m have been represented in the supplementary file (see Table 3-a, Table 3-b, Table 3-c and Table 3-d). The best solutions have been achieved after 200 independent runs for the three SA models. The simulation has been done for three kinds of ground systems including ideal grounding system, rod-shaped and counterpoise-shaped systems and different soil resistivities. As can be seen, optimum parameter values are different from the initial values that are shown in Table 2. The optimum values have been calculated based on the error minimization between the datasheet and the simulated residual voltage for all considered grounding systems (ideal, counterpoise and rod). It is obvious that the considering grounding system model affects the computed optimal parameter values.

Also, it is obvious that soil with different resistivities influences the optimized parameters which shows the effect of soil resistivity on the SA model parameters. Although the effect of the grounding system on the SA performances may differ and sometimes the counterpoise system may be better than a single rod, or vice versa, but the important issue is that if an SA is installed in a power system for insulation coordination studies, the SA parameters should be optimized according to the considered ground system in the studied system. In this case, the surge residual voltage is matched with the manufacture reported

Table 1.
SA electrical and insulation information

Maximum continuous operating voltage		120 kV
Rated voltage		150 kV
Maximum residual voltage with lightning current 8/20 μs	5 kA	367 kV
	10 kA	396 kV
	20 kA	449 kV
Maximum residual voltage with lightning current 1/20 μs	10 kA	430 kV
Height		1330 mm
Creepage distance		3320 mm

Table 2.
SA model parameters primary values

Parameters	IEEE	Pinceti-Giannettoni	Fernandez–Diaz
L_1 (μH)	19.95	3.21	0.48
R_1 (Ω)	86.45	–	–
L_0 (μH)	0.267	1.07	–
R_0 (Ω)	133	1000000	1000000
C (pF)	75.2	–	75.18

Table 3.
Optimum values of SA model parameters after objective function minimization ($\rho = 100\ \Omega$ m)

Model	IEEE			Pinceti–Giannettoni			Fernandez–Diaz		
Parameters	Ideal ground	Counterpoise	Rod	Ideal ground	Counterpoise	Rod	Ideal ground	Counterpoise	Rod
L_1 (μH)	16.25	17.49	18.25	8	5	2.25	0.1	0.09	0.2
R_1 (Ω)	72.36	59.69	55.82	–	–	–	–	–	–
L_0 (μH)	0.252	0.233	0.1304	0.3	2.94	2	–	–	–
R_0 (Ω)	142.8	107.2	133	1000000	1031000	1045700	800000	700000	700000
C (pF)	73.22	75.9	78.2	–	–	–	30	20	40

residual voltage, resulting in a more reliable SA model. To show the grounding system effect on the SA residual voltage, the simulated residual voltage of optimized and nonoptimized model is shown in Figure 3. In these conditions, 5 kA 8/20 μs lightning current has been applied to SA IEEE model. The soil resistivity has been elected 500 Ω m for rod grounding system. As shown in Figure 3, considering grounding system impedance influences the residual voltage, and the optimum values of the SA model parameters lead to more precise results. The simulated residual voltage for optimized SA model has less difference compared to simulation one.

The simulated residual voltage curves for rod and counterpoise grounding system and for optimized SA model are shown in Figure 4. In this condition, 10 kA 8/20 μs lightning current has been applied to the IEEE model of SA, and the soil resistivity has been chosen 500, 1000 and 3000 Ω m. The measured residual voltage for 10 kA 8/20 μs lightning surge has been shown in Figure 5. The residual voltage measuring has been carried out in the laboratory with the ground system including the rod with the length of the 6 m and 8 mm circular cross-sectional radius. In addition, the soil resistivity was 100 Ω m. To validate the simulation, simulated surge residual voltage for rod grounding system and 100 Ω m resistivity has been shown in Figure 5. As shown in Figure 5, simulated residual voltage and measured one are matched for optimum SA frequency model.

In addition, comparing Figures 4 and 5 shows that the obtained residual voltage has good agreement with the measured signal, and the optimization process was able to predict SA frequency model parameters with acceptable accuracy. The residual voltage peak values for rod grounding system are 396, 402 and 404 kV for 500, 1000 and 3000 Ω m, respectively. These values for counterpoise grounding system are 397, 398 and 400 kV for 500, 1000 and 3000 Ω m, respectively. As shown in this figure, the grounding system type can affect the residual voltage amplitude, and it is better to consider the grounding system impedance during SA modeling.

Figure 6 shows the PSO-GWO algorithm convergence diagram for the three studied models' best solution for 10 kA, 8/20 μs injected current and counterpoise system. In this figure, soil resistivity is 100 Ω m. The initial values of peak residual voltage which have been obtained by the represented parameters in Table 2 have been shown in Table 4 for soil resistivity 100 Ω m. The obtained results for other soil resistivity have been represented in the supplementary file (see Table 4-a to Table 4-d).

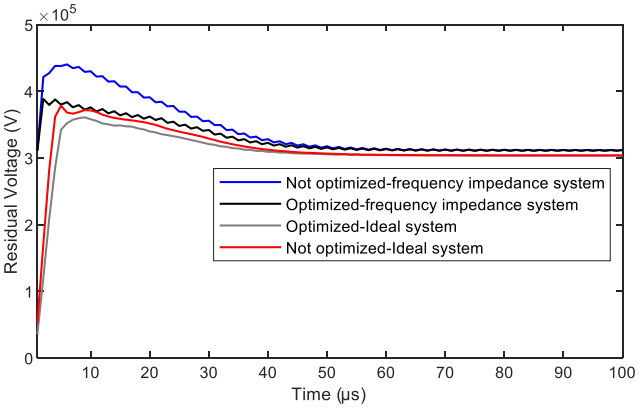

Figure 3.
The simulated residual voltage of optimized and nonoptimized surge arrester model

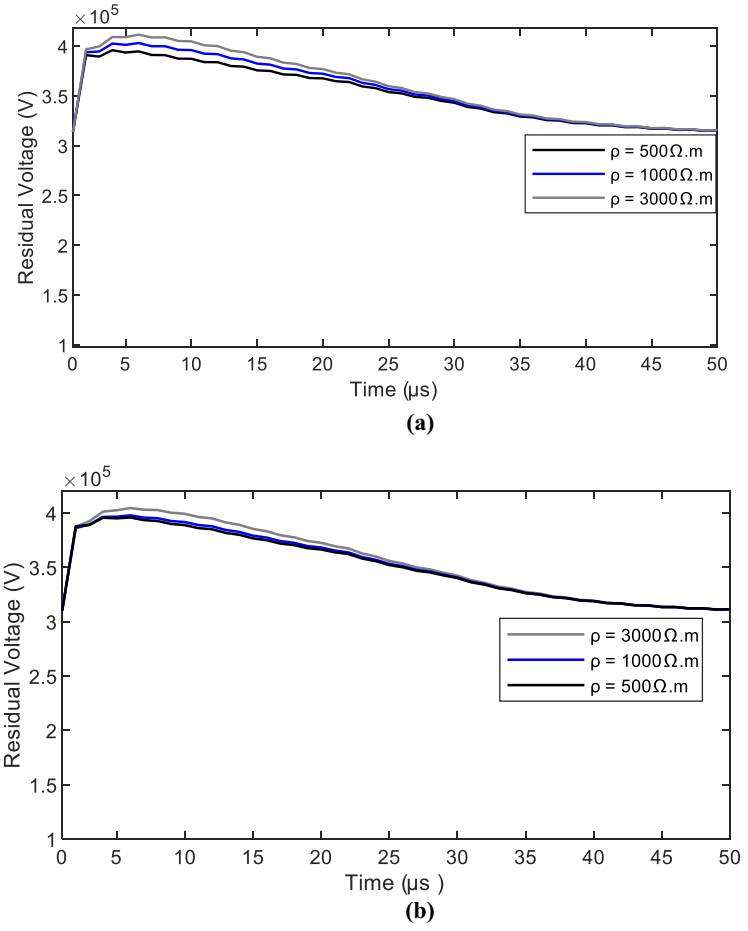

Figure 4.
Surge arrester residual voltage for rod and counterpoise grounding systems

Notes: (a) Rod; (b) counterpoise

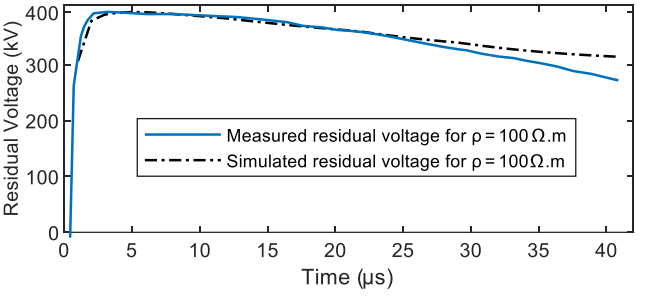

Figure 5.
Surge arrester measured and simulated residual voltage curves

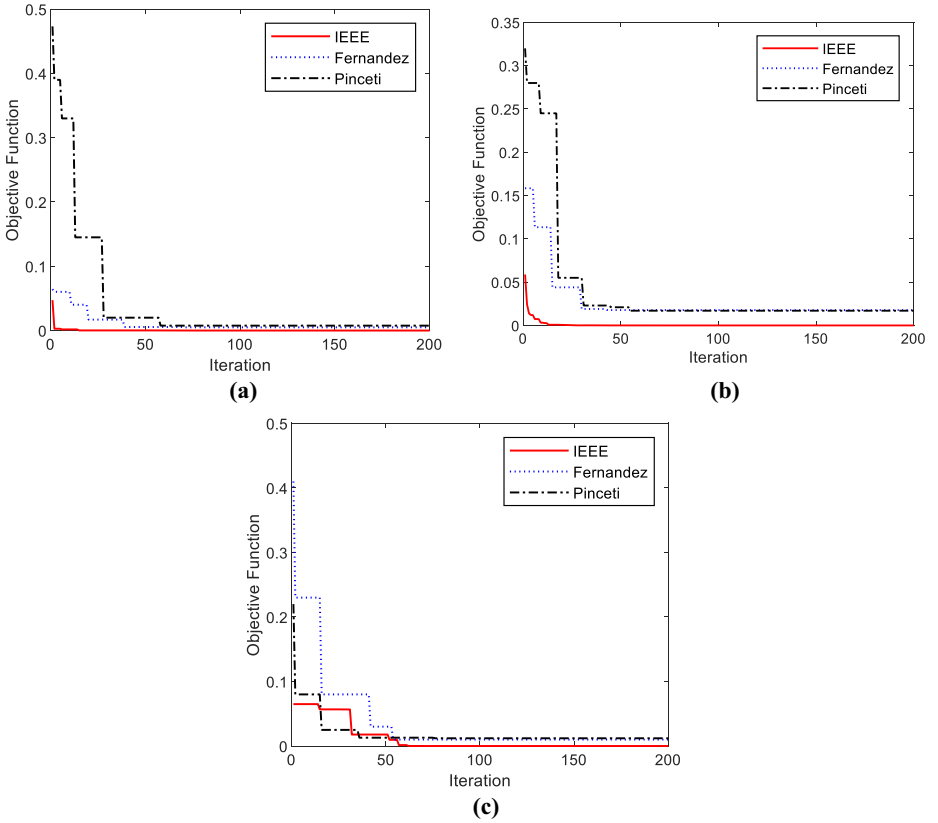

Notes: (a) Ideal ground; (b) counterpoise; (c) rod (ρ = 100 Ω m)

Figure 6.
The PSO-GWO algorithm convergence diagram

As can be seen in Table 4, the residual voltage peak values are different for the current values of 5, 10 and 20 kV. The presented results show that the grounding frequency-dependent model can change the residual voltage compared to the ideal ground condition. Based on the obtained results from Table 4, for the ideal ground system, the relative errors maximum value of the IEEE model occurs in 10 kA, 1/20 μs lightning impulse current which is equal to 6.1%. This error for the Pinceti model is 6.4% and has been happened in 20 kA, 8/20 μs. Moreover, this value for the Fernandez model takes place in 5 kA lightning impulse current, and it is equal to 8.17%. For the rod-shape and the counterpoise-shape, the Fernandez model has the lowest relative error for 5 kA, 8/20 μs and 10 kA, 8/20 μs current waveforms, in which the finest (lowest) relative error for 10 kA, 1/20 μs and 20 kA, 8/20 μs has been obtained by the Pinceti model. In addition, the IEEE model has the worst performance in terms of minimum and maximum amplitudes of relative error.

Based on the obtained results from Supplementary Table 4-a, for the soil resistivity 250 Ω m, the relative errors maximum value of the IEEE model occurs in 5 kA, 8/20 μs lightning impulse current which is equal to 15.3%. This error for the Pinceti model is 8.14% and has been occurred in 10 kA, 1/20 μs. Moreover, this value for the Fernandez model takes

Table 4.
The initial amplitude of residual voltage (in kV) for each SA model (ρ = 100 Ω m)

Model		IEEE			Pinceti–Giannettoni			Fernandez–Diaz	
Parameters	Ideal ground	Rod	Counterpoise	Ideal ground	Rod	Counterpoise	Ideal ground	Rod	Counterpoise
$Vs_{,10kA(1/20\mu s)}$	456.1	471.8	466.75	431	442	437.5	420.5	436.5	432.2
Error%	6.1	9.7	8.5	0.232	2.8	1.74	–2.2	1.4	0.51
$Vs_{,5kA(8/20\mu s)}$	380	409.15	400	355	364.5	360	397	407	411.6
Error%	3.54	11.4	8.99	–3.2	–0.68	–1.9	8.17	10.8	12.1
$Vs_{,10kA(8/20\mu s)}$	411	421.4	417	372.5	383	378.5	413	428.2	424.2
Error%	3.79	6.41	5.03	–5.93	–3.28	–4.42	4.3	8.13	7.12
$Vs_{,20kA(8/20\mu s)}$	462	480	473.5	420	439	434	439	457	462
Error%	2.89	6.9	5.45	–6.4	–2.22	–3.3	–2.22	1.7	2.89

place in 5 kA lightning impulse current, and it is equal to 13.9%. Based on the reported results in Supplementary Table 4-b, for the soil resistivity 500 Ω m, the maximum error values of the IEEE model, Pinceti model and Fernandez model are equal to 19.2, 13.76 and 15.2%, respectively.

Based on the obtained results from Supplementary Table 4-c, the maximum error value for the IEEE model is 9.3% and has been happened in 10 kA, 1/20 μs. Moreover, this value for the Fernandez model takes place in 20 kA lightning impulse current and it is equal to −9.1%. The highest error for Pinceti is 9.06%. As shown in Supplementary Table 4-d, the IEEE model has the maximum error value compared to two other models. This error takes place for 20 kA, 8/20 μs and the amplitude is 14.25%.

The peak residual voltage optimum values based on the optimized parameters, which have been given in Table 3, have been represented in Table 5. As shown in Table 5, for soil resistivity 100 Ω m (compared to results in Table 3), the better results for lightning impulse currents (8/20-μs waveform) and steep front surge (1/2-μs waveform) have been achieved after the optimization process. The best relative error values for the injected transient current have been obtained by the Pinceti model for all represent grounding systems. For lightning impulse current, the IEEE model has the best result and the lowest relative error values compared to the Fernandez and Pinceti models.

The IEEE model parameters optimization reduces the maximum error of the residual voltage by about 5.5% compared to the initial value for the ideal ground. The error reductions for the rod and the counterpoise systems are 10% and 8.1% compared to initial values, respectively. Comparison of the Pinceti model parameters maximum error before and after optimization shows that the maximum error has been reduced by 7.2% for the ideal ground. The error reduction for the rod and the counterpoise systems is 4.7% and 5%, respectively. Under such conditions, the error reductions are 7.6%, 10.6% and 9.5% for the ideal, rod and the counterpoise grounds in the Fernandez model.

The obtained result for other soil resistivities has been represented in the supplementary file (see Table 5-a to Table 5-d). Comparing the represented results of Table 5-a to Table 5-d with Table 4-a to Table 4-d shows that the obtained errors have been improved for the different considered soil resistivities. These results indicate that the grounding impedance should be modeled for the dynamic model parameters computation. It leads to fewer errors and more accurate results. Results show that the grounding system frequency behavior has effects on the SA optimum values parameter. This shows the importance of a frequency-dependent model representation for SA parameters estimation.

To compare the efficiency of the PSO-GWO, the obtained results for 10 kA, 8/20 μs have been compared to the other optimization techniques results. It should be noted that all investigations, in previous researches, have been performed for an ideal grounding system, and the grounding system resistance effect has not been investigated in previous literatures. The best-estimated parameters for the IEEE model and soil resistivity 100 Ω m have been listed in Table 6. It should be mentioned that GA is an effective technique for optimization problems. The concept is easy to understand, but GA is a time-consuming method.

In accordance with above explanation and as shown in Table 6, the PSO-GWO algorithm has predicted the estimated parameters more accurately than the other algorithms. The lowest error for the residual voltage amplitude of the SA model has been achieved by PSO-GWO algorithm. Besides, the modified PSO had the best results compared to the genetic and the PSO

Table 5.
Residual voltage optimized value (in kV) for each model of SA (ρ = 100 Ω m)

Model		IEEE			Pinceti–Giannettoni			Fernandez–Diaz	
Parameters	Ideal ground	Rod	Counterpoise	Ideal ground	Rod	Counterpoise	Ideal ground	Rod	Counterpoise
$Vs_{,10kA(1/20\mu s)}$	431	430.5	430.2	431	430.5	429.8	428.5	431.6	429.7
Error %	0.232	0.11	0.465	0.23	0.115	–0.0465	–0.348	0.372	0.69
$Vs_{,5kA(8/20\mu s)}$	367.1	368.1	367.5	363	366	365.3	367.4	368.15	367.7
Error %	0.0272	0.299	0.136	1.08	–0.272	–0.463	0.1	0.31	0.19
$Vs_{,10kA(8/20\mu s)}$	396.00000733	395.9	396.3	399	402.35	396.5	398	403	400
Error %	$1.85e^{-6}$	–0.02	0.07	0.76	1.7	0.12	0.51	1.77	1
$Vs_{,20kA(8/20\mu s)}$	449.31	449.04	449.01	448.13	449.41	448.7	444	449.29	449.1
Error %	0.069	0.0088	0.0022	–0.193	0.0913	–0.066	–1.11	0.064	0.022

Table 6.
IEEE Model optimum results based on PSO-GWO and PSO techniques (ρ = 100 Ω m)

Injected current 10kA(8/20μs)	PSO-GWO IEEE Ideal ground	PSO-GWO IEEE Counterpoise	PSO-GWO Rod	Modified PSO (Vahidi *et al.*, 2008) IEEE Ideal ground	Modified PSO (Vahidi *et al.*, 2008) IEEE Counterpoise	Modified PSO (Vahidi *et al.*, 2008) Rod
L_1 (μH)	16.25	17.49	18.25	15.68	15	15.003
R_1 (Ω)	72.36	59.69	55.82	55.533	45	50
L_0 (μH)	0.252	0.233	0.1304	0.1	0.1896	0.10084
R_0 (Ω)	142.8	107.2	133	100.4536	120.59	137.088
C (pF)	73.22	75.9	78.2	75.722	76.528	70.734
$Vs_{,10kA(8/20\mu s)}$	396.00000733	396.3	395.9	399.88	405.126	409.26
Error%	$1.85e^{-6}$	0.07	–0.02	0.0979	2.3	3.34
Injected current 10 kA(8/20μs)	PSO (Christodoulou *et al.*, 2011) IEEE Ideal ground	PSO (Christodoulou *et al.*, 2011) IEEE Counterpoise	PSO (Christodoulou *et al.*, 2011) Rod	Genetic algorithm (Martinez and Durbak, 2005) IEEE Ideal ground	Genetic algorithm (Martinez and Durbak, 2005) IEEE Counterpoise	Genetic algorithm (Martinez and Durbak, 2005) Rod
L_1 (μH)	16	15.2	14.98	17	15	15.003
R_1 (Ω)	54	43	52	57	45	50
L_0 (μH)	0.1	0.193	0.999	0.11	0.1896	0.10084
R_0 (Ω)	99.54	117	136.23	102.243	120.59	137.088
C (pF)	74.22	76.9	72.2	76.02	76.528	70.734
$Vs_{,10kA(8/20\mu s)}$	401	406.71	411.3	401.5	407.23	411.29
Error%	1.26	2.7	3.86	1.39	2.83	3.86

techniques. The comparative performances of the studied algorithms for the minimum and maximum repetitions and simulation times have been summarized in Table 7.

As shown in Table 7, it is obvious that PSO-GWO is able to solve a proposed problem with lower errors, the most of the time as compared to the PSO and GA. To show the convergence ability of the PSO-GWO, the convergence performances of these algorithms have been compared together, and the achieved results have been represented in Figure 7. On the basis of obtained results and convergence performance of the variants, it is concluded that PSO-GWO is more reliable in giving superior quality results with reasonable iterations and avoids premature convergence of the search process to local optimal point and provides superior exploration of the search course.

6. Conclusions

This paper focuses on the inclusion of the frequency behavior of grounding system effect on SA model parameters estimation. SA modeling was performed both for the ideal grounding system and frequency-dependent grounding system and for various soil resistivities. A PSO-GWO algorithm was developed to determine the parameters of metal oxide SA model, including the IEEE, Pinceti–Giannettoni and Fernandez–Diaz. The results show that the frequency behavior of the grounding system affects the optimum values of the SA parameters. Depending on the grounding system types and soil resistivity, different parameter values for SA dynamic model have been acquired. Consequently, the SA parameters have been calculated more accurately when the frequency behavior of the grounding system is considered in the dynamic model. This is an important issue especially for insulation coordination studies. Finally, to compare the efficiency of the PSO-GWO, the obtained results based on the optimization method

Table 7. Comparative performances of PSO-GWO and PSO algorithms for IEEE model

Algorithm	Run no.	Error average	Error variance	Minimum error	Maximum error	Simulation time (min)
PSO-GWO Modified	50	0.0092	8.1e-5	1.85e-6	0.09	2.54
PSO	50	0.046	1.98	0.00886	0.12	2.38
PSO	50	0.055	2.05	0.014	0.143	1.55
GA	50	0.059	2.31	0.016	0.156	1.46

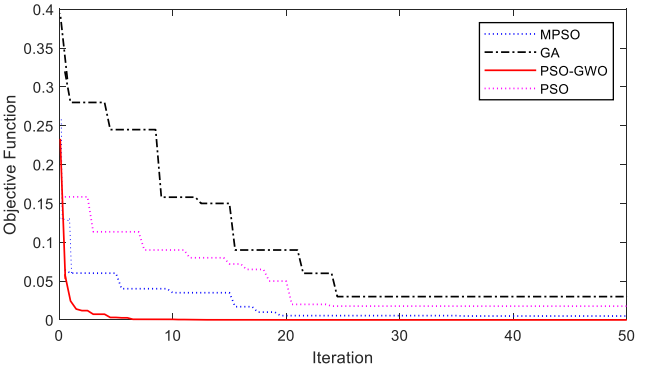

Figure 7. Convergence curve of studied optimization algorithms for IEEE model

have been compared to the other optimization techniques. The results showed that the proposed optimization algorithm achieved the lowest error, which is better than the one provided by other investigated algorithms.

References

Application of Surge Protective Devices Subcommittee (2023), "Modeling of metal oxide surge arresters", *IEEE* working group 3.4.11.

Bayadi, A. (2008), "Parameter identification of ZnO surge arrester models based on genetic algorithms", *Electric Power Systems Research*, Vol. 78 No. 7, pp. 1204-1209.

Bedoui, S. and Bayadi, A. (2019), "Insulation coordination study of 400 kV high voltage substation, in", *2019 Algerian Large Electrical Network Conference (CAGRE)*, *IEEE*, pp. 1-6.

Christodoulou, C.A., Gonos, I.F. and Stathopulos, I.A. (2011), "Estimation of the parameters of metal oxide gapless surge arrester equivalent circuit models using genetic algorithm", *Electric Power Systems Research*, Vol. 81 No. 10, pp. 1881-1886.

Christodoulou, C.A., Ekonomou, L., Papanikolaou, N. and Gonos, I.F. (2014), "Effect of the grounding resistance to the behaviour of high-voltage transmission lines' surge arresters", *IET Science, Measurement and Technology*, Vol. 8 No. 6, pp. 470-478.

Christodoulou, C.A., Ekonomou, L., Mitropoulou, A.D., Vita, V. and Stathopulos, I.A. (2010a), "Surge arresters' circuit models review and their application to a Hellenic 150 kV transmission line", *Simulation Modelling Practice and Theory*, Vol. 18 No. 6, pp. 836-849.

Christodoulou, C.A., Vita, V., Ekonomou, L., Chatzarakis, G.E. and Stathopulos, I.A. (2010b), "Application of Powell's optimization method to surge arrester circuit models' parameters", *Energy*, Vol. 35 No. 8, pp. 3375-3380.

Esmin, A.A., Lambert-Torres, G. and De Souza, A.Z. (2005), "A hybrid particle swarm optimization applied to loss power minimization", *IEEE Transactions on Power Systems*, Vol. 20 No. 2, pp. 859-866.

Faris, H., Aljarah, I., Al-Betar, M.A. and Mirjalili, S. (2018), "Grey wolf optimizer: a review of recent variants and applications", *Neural Computing and Applications*, Vol. 30 No. 2, pp. 413-435.

Fernandez, F. and Diaz, R. (2001), "Metal oxide surge arrester model for fast transient simulations", *Proceedings of 2001 International Conference on Power System Transients*, Citeseer, pp. 681-687.

Gaing, Z.-L. (2003), "Particle swarm optimization to solving the economic dispatch considering the generator constraints", *IEEE Transactions on Power Systems*, Vol. 18 No. 3, pp. 1187-1195.

Jacqmaer, P., Driesen, J. and Geuzaine, C. (2009), "Modelling earthing systems and cables with moment methods", *COMPEL – The International Journal for Computation and Mathematics in Electrical and Electronic Engineering*, Vol. 28 No. 4, pp. 989-1004.

Khodsuz, M. (2022), "Externally gapped line arrester performance in high voltage transmission line using frequency grounding system: absorbed energy and expected life assessment", *IET Science, Measurement and Technology*, Vol. 16 No. 7, pp. 426-440.

Li, Z.-X., Li, P. and Wang, K.-C. (2021), "Transient lightning response to grounding grids buried in horizontal multilayered earth model considering time domain quasi-static complex image method and soil ionization effect", *COMPEL – The International Journal for Computation and Mathematics in Electrical and Electronic Engineering*, Vol. 40 No. 3, pp. 516-534.

Lira, G.R.S., Fernandes, D. and Costa, E.G. (2009), "Parameter identification technique for a dynamic metal-oxide surge arrester model", *International Conference on Power Systems Transients*.

Longmire, C.L. and Smith, K.S. (1975), *A Universal Impedance for Soils*, Mission Research Corp, Santa Barbara, CA.

Mahapatra, S., Badi, M. and Raj, S. (2019), "Implementation of PSO, it's variants and hybrid GWO-PSO for improving reactive power planning", *2019 Global Conference for Advancement in Technology (GCAT)*, *IEEE*, pp. 1-6.

Martinez, J.A. and Durbak, D.W. (2005), "Parameter determination for modeling systems transients-Part V: Surge arresters", *IEEE Transactions on Power Delivery*, Vol. 20 No. 3, pp. 2073-2078.

Mirjalili, S., Mirjalili, S.M. and Lewis, A. (2014), "Grey wolf optimizer", *Advances in Engineering Software*, Vol. 69, pp. 46-61.

Nafar, M., Gharehpetian, G.B. and Niknam, T. (2011), "Improvement of estimation of surge arrester parameters by using modified particle swarm optimization", *Energy*, Vol. 36 No. 8, pp. 4848-4854.

Nafar, M., Gharehpetian, G.B. and Niknam, T. (2012), "Comparison of the parameter estimation methods of surge arresters using modified particle swarm optimization algorithm", *European Transactions on Electrical Power*, Vol. 22 No. 8, pp. 1146-1160.

Niknam, T., Meymand, H.Z. and Nayeripour, M. (2010), "A practical algorithm for optimal operation management of distribution network including fuel cell power plants", *Renewable Energy*, Vol. 35 No. 8, pp. 1696-1714.

Pal, D., Verma, P., Gautam, D. and Indait, P. (2016), "Improved optimization technique using hybrid ACO-PSO", *2016 2nd International Conference on Next Generation Computing Technologies (NGCT)*, *IEEE*, pp. 277-282.

Pinceti, P. and Giannettoni, M. (1999), "A simplified model for zinc oxide surge arresters", *IEEE Transactions on Power Delivery*, Vol. 14 No. 2, pp. 393-398.

Rokbani, N., Abraham, A. and Alimi, A.M. (2013), "Fuzzy ant supervised by PSO and simplified ant supervised PSO applied to TSP", *13th International Conference on Hybrid Intelligent Systems (HIS 2013)*, *IEEE*, pp. 251-255.

Sajadi, S.S., Ostadzadeh, S.R. and Sadeghi, S.H.H. (2020), "Parametric dependence of lightning impulse behavior of grounding electrodes buried in a dispersive and ionized lossy soil under first-and subsequent-stroke currents", *COMPEL – The International Journal for Computation and Mathematics in Electrical and Electronic Engineering*, Vol. 39 No. 4, pp. 757-773.

Sengmanivanh, P., Hongesombut, K., Punyakunlaset, S., Rerkpreedapong, D. and Romphochai, S. (2021), "Cost-effective insulation coordination design for 115-kV transmission line due to lightning back flashover", *2021 18th International Conference on Electrical Engineering/Electronics, Computer, Telecommunications and Information Technology (ECTI-CON)*, *IEEE*, pp. 56-59.

Shariatinasab, R. and Gholinezhad, J. (2017), "The effect of grounding system modeling on lightning-related studies of transmission lines", *Journal of Applied Research and Technology*, Vol. 15 No. 6, pp. 545-554.

Shariatinasab, R., Gholinezhad, J. and Sheshyekani, K. (2017), "Estimation of energy stress of surge arresters considering the high-frequency behavior of grounding systems", *IEEE Transactions on Electromagnetic Compatibility*, Vol. 60 No. 4, pp. 917-925.

Sheshyekani, K., Akbari, M., Tabei, B. and Kazemi, R. (2014), "Wideband modeling of large grounding systems to interface with electromagnetic transient solvers", *IEEE Transactions on Power Delivery*, Vol. 29 No. 4, pp. 1868-1876.

Subcommittee, A.O.S.P.D. (1992), "Modeling of metal oxide surge arresters ieee working group 3.4. 11 application of surge protective devices subcommittee surge protective devices committee".

Vahidi, B., Mousavi Aghah, S.M. and Moaddabi Pirkolachahi, N. (2008), "Optimum parameter identification technique of metal oxide surge arrester model using genetic algorithm", *International Review of Electrical Engineering*, Vol. 10 No. 1.

Visacro, S., Alipio, R., Vale, M.H.M. and Pereira, C. (2011), "The response of grounding electrodes to lightning currents: the effect of frequency-dependent soil resistivity and permittivity", *IEEE Transactions on Electromagnetic Compatibility*, Vol. 53 No. 2, pp. 401-406.

Zeinoddini-Meymand, H., Vahidi, B., Naghizadeh, R.A. and Moghimi-Haji, M. (2013), "Optimal surge arrester parameter estimation using a PSO-based multiobjective approach", *IEEE Transactions on Power Delivery*, Vol. 28 No. 3, pp. 1758-1769.

Zhao, H. and Magoulès, F. (2012), "A review on the prediction of building energy consumption", *Renewable and Sustainable Energy Reviews*, Vol. 16 No. 6, pp. 3586-3592.

Zhou, Y., Xie, Y., Zhang, D., Dong, N., Chen, Y. and Jing, Y. (2020), "Response of 10-kV metal-oxide surge arresters excited by nanosecond-level transient electromagnetic disturbances", *IEEE Transactions on Electromagnetic Compatibility*, Vol. 63 No. 2, pp. 614-621.

Supplementary material

The supplementary material for this article can be found online.

Corresponding author

Masume Khodsuz can be contacted at: m.khodsouz@mazust.ac.ir